Received: 22 August 2023 | Revised: 22 December 2023 | Accepted: 26 December 2023

DOI: 10.1002/pol.20230613

RESEARCH ARTICLE

JOURNAL OF POLYMER SCIENCE WILEY

Biosourced spherical microbeads from brewer's spent grain for sustainable personal hygiene products

Amy McMackin[1,2] | **Vincent Banville**[2] | **Sébastien Cardinal**[1]

[1]Département de Biologie, Chimie et Géographie, Université du Québec à Rimouski (UQAR), Rimouski, Québec, Canada

[2]Centre de Développement Bioalimentaire du Québec, Sainte-Anne-de-la-Pocatière, Québec, Canada

Correspondence
Sébastien Cardinal, Département de Biologie, Chimie et Géographie, Université du Québec à Rimouski (UQAR), Rimouski, QC, Canada.
Email: sebastien_cardinal@uqar.ca

Funding information
Mitacs, Grant/Award Number: IT20615; Ministère de l'Agriculture, des Pêcheries et de l'Alimentation, Grant/Award Number: IA119014

Abstract

Many countries have recently banned the production and importation of petrochemical plastic microbeads for use as exfoliating agents in personal care products. Plastic particles in products of this nature are too small to be retrieved during wastewater treatment and they accumulate in the environment, negatively impacting living organisms and ecosystems. Sustainable alternatives that offer comparable mechanical properties to synthetic plastic microbeads could be developed using biowaste material. Brewer's spent grain (BSG), the primary residue of the brewery industry, is shown herein to be a promising starting material in the development of biodegradable, nontoxic microbeads. After dilute acid hydrolysis, pretreated lignocellulosic pulp from BSG is solubilized using an aqueous system of NaOH and ZnO. Solid microbeads may then be formed by dropping the resulting solution into an acid bath, filtering, and drying. The conditions of each step required optimization to successfully produce spherical microbeads with a mean diameter as small as 1.25 mm, a homogeneous size distribution, and an average hardness of 199 MPa. The beads also demonstrated superior cleansing abilities to commercially available natural exfoliating particles. BSG microbeads are therefore a promising option for use as a physical exfoliating agent in various personal hygiene products.

KEYWORDS

Brewer's spent grain, cellulose, green chemistry, polymers, waste valorization

1 | INTRODUCTION

The world is shaped by plastics to the extent that their presence has become the indicator of a new geological era.[1,2] Plastics' durability is one of the reasons for their widespread use but leads to their persistence in the environment. Microplastics, particles less than 5 mm in diameter,[3,4] are of particular concern as there is no feasible method for their complete retrieval from the environment.[5–7] Marine environments especially bear the consequences of plastic pollution, with conservative estimates placing 14 million tonnes of microplastics on the ocean floor alone,[8,9] not to mention the particles suspended in the water column. Due to their small size, microplastics may be ingested at all levels of the food chain and are known contaminants of human food and drinking water sources.[10,11] They also leach the chemical additives they contain and transport toxic chemicals (such as persistent organic pollutants and heavy metals), which bioaccumulate as they are ingested and transferred up the food chain.[11,12]

Microplastics can be grouped into two categories, primary and secondary, according to their origin. While secondary microplastics result from the decomposition of larger plastic items, primary microplastics are produced at these sizes for use in a variety of commercial applications.[3] One such application is as a physical exfoliating agent in personal hygiene products, such as soaps, scrubs, and toothpaste—products designed to be washed down the drain during use.[13,14] Wastewater treatment facilities can remove the majority of these beads; still, a significant fraction escapes filtration and ends up accumulating in aquatic environments.[15–17] Consequently, plastic microbeads have recently been banned or voluntarily phased out in many countries,[18] motivating researchers and industry members alike to explore sustainable alternatives.

Plastic microbeads for personal hygiene products have conventionally been made from polyethylene (PE), polyester (PES), polyvinyl chloride (PVC), polypropylene (PP), and polystyrene (PS) as these are low-cost materials with desirable mechanical characteristics.[13,17,19–21] A 2021 study by researchers at the Korea Research Institute of Chemical Technology (KRICT) lists three classes of biodegradable alternatives: natural abrasive materials, bio-based synthetic polymers, and natural polymers.[22] Figure 1 compares the life cycle of these to that of conventional plastic microbeads.

Examples of each class of materials are currently used in personal hygiene products but exhibit noteworthy drawbacks. Naturally hard materials, like stone fruit pits or aluminum oxide, need to be ground down to meet the required dimensions, resulting in sharp, irregular particles.[23,24] Accordingly, personal hygiene products containing these abrasives are not recommended for use on sensitive skin,[23,25] restricting their widespread use in personal hygiene products. Bio-based synthetic polymers, such as polylactic acid (PLA), can be liquefied and easily shaped into uniform, spherical microbeads with adequate hardness.[26–28] However, these processes commonly rely on the use of expensive ionic liquids or organic solvents,[26,27,29] and rates of biodegradation are so slow and condition-specific that these microbeads may have even greater environmental consequences than their petrochemical-based analogs.[30] Natural polymers can also be suspended in solutions that can be readily shaped and solidified into microbeads but may also require costly or toxic processing conditions.[31–36] Moreover, their starting materials are commonly coveted by other industries,[37,38] and their mechanical properties tend to be lower than other proposed alternatives.[26,39] Interestingly, microbeads made from chitosan obtained from crustacean waste were recently proposed as a promising option: these beads are inexpensive to produce, use noncytotoxic cross-linkers, and present the characteristics required of mechanical exfoliating agents.[22] However, their animal-based nature restricts their use in the cosmetics industry, which is increasingly turning toward plant-based formulations that reduce the likelihood of allergic reactions.

Cellulose, the most abundant polymer in nature, has been extensively investigated as a biodegradable building block for new materials, including microbeads.[35,40–43] Pretreated cellulose fibers can be dissolved in a limited choice of solvents, such as certain ionic liquids or aqueous alkali solutions.[35,44,45] Beads can be shaped by dropping, spraying, or membrane emulsification techniques, among others, and the polymeric structure is solidified by the regeneration of the polymeric structure's hydrogen bonding network.[41,42] While these microbeads are desirable for many applications (notably functional foods, pharmaceutical uses, and biomedical applications),[34,40–43] they generally lack the hardness required of exfoliating microbeads. Lignin, another abundant natural polymer, can be added to these systems to create composite lignin-cellulose microbeads, as it can be dissolved and regenerated using the same solvent and anti-solvent systems as cellulose,[46–48] or can be used alone.[49] Cellulose-lignin or pure lignin microbeads have increased hardness,[50] as well as potential antioxidant and antimicrobial properties.[28,46,50] Lignin also shows an affinity for adsorbing organic contaminants and metal ions.[46]

Meanwhile, the global brewery industry generates an estimated 39 million tonnes of undervalued residual lignocellulosic biomass annually.[51] This residue, known as brewer's spent grain (BSG), is the primary by-product of beer production, accounting for approximately 85% of the process's total waste.[52] Having previously been seen as having little added value, the main use of BSG is as a component of animal feed, with each metric ton being sold to farmers at an approximate cost of $40 (USD).[53] Major challenges to using BSG as a starting material in more valuable industrial applications are its variable molecular composition (depending on the precise conditions used in the brewing process and the exact cereal blend used) and its high humidity. In general, the solid mass fraction of BSG contains 16%–25% cellulose, 21%–28% hemicellulose, 11%–27% lignin, 15%–24% proteins, 2%–4% ash, and around 10% soluble matter.[54] Humidity commonly represents between 77 and 85% of the total weight of the biomass.[54,55]

Herein, we sought to valorize BSG by developing a process to produce biodegradable exfoliating microbeads with mechanical properties and stability in compliance with requirements for use in personal hygiene products. Sourcing cellulose and lignin directly from BSG reduces the environmental strain associated with extracting and purifying these natural polymers from biomass to produce similar cellulose and/or lignin microbeads. We also theorized that the other components present in BSG could positively contribute to the total solids content in the final beads. Despite the

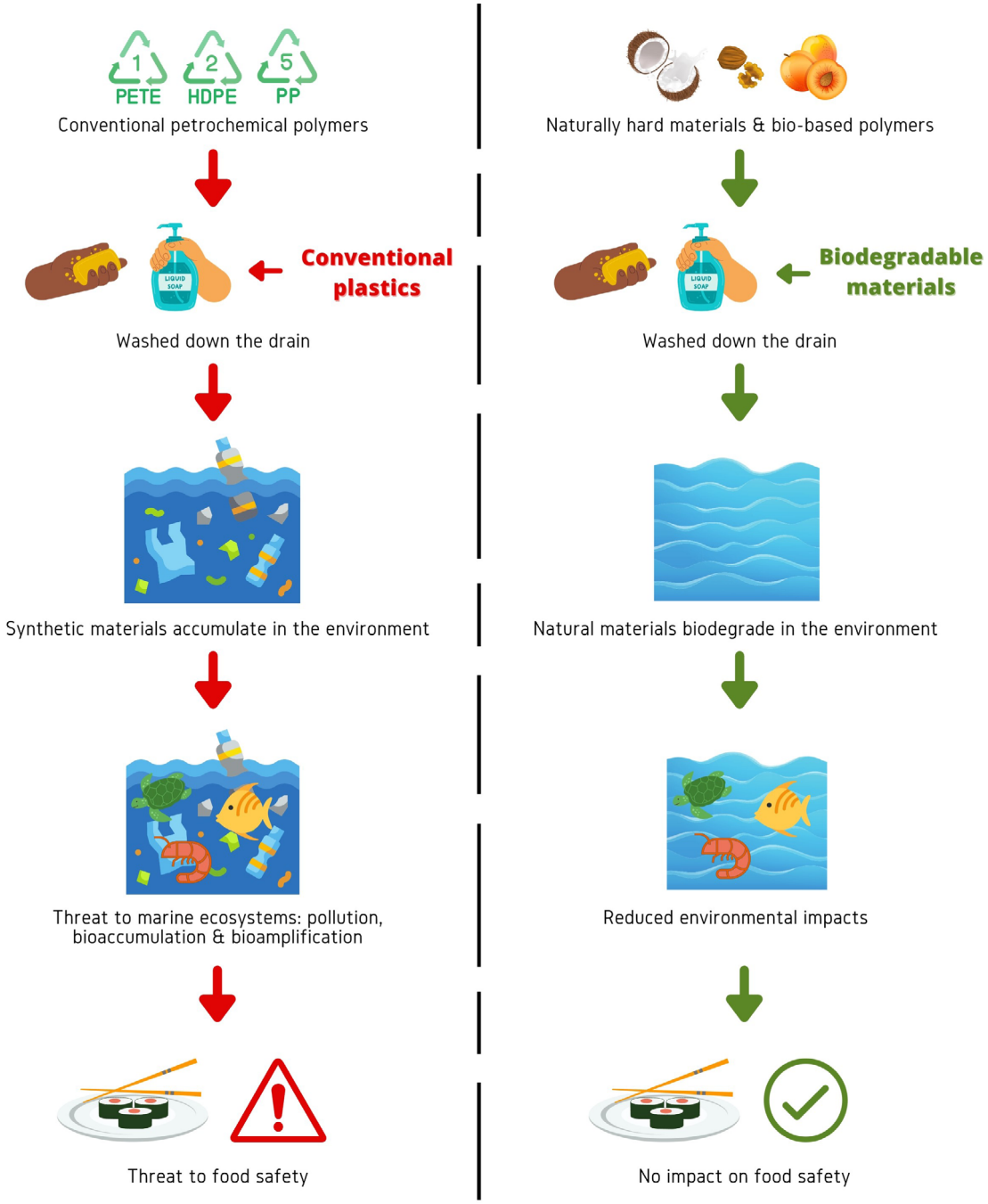

FIGURE 1 Schematization of the typical life cycle of conventional plastic microbeads versus biodegradable alternatives when used in personal hygiene products. Graphic inspired by the work of Ju et al.[22]

variable composition and humidity of BSG, we sought to develop a method that does not require drying or biomass composition uniformization before further processing. After developing a reliable protocol to produce BSG microbeads, we characterized the final product to ensure it conforms to industry requirements. Notably, we tested the beads' mechanical properties and stability in various personal hygiene product matrices, concluding that BSG microbeads provide an alternative to conventional plastics and provide a novel use for undervalued biomass.

2 | RESULTS AND DISCUSSION

2.1 | Preparation of brewer's spent grain microbeads

2.1.1 | General

Brewer's spent grain (BSG)-based microbeads are produced by following three distinct steps: pretreatment, BSG solubilization, and shaping and solidification. To

determine the best conditions, we modified one system parameter at a time. These experiments were realized on a single batch of BSG; the reproducibility of the optimized method for BSG of different compositions was evaluated afterward on samples obtained from different batches. Quantities of BSG used to prepare the samples are reported on a dry solids basis, not as a function of the total weight of humid biomass in the sample.

2.1.2 | Pretreatment

Although pretreatment adds a step to the overall process, it proved to be a critical first step in the solubilization of the grain and the subsequent production of BSG microbeads. Using work on the enhancement of cellulose dissolution by acid hydrolysis as inspiration,[56] we evaluated the trituration of BSG in aqueous solutions of HCl.

Dilute acid solution concentration was varied between 0.23, 0.45, and 0.60 M. Acid hydrolysis was evaluated at 50, 75, and 90°C. Pretreatment duration varied, with tests at 0.5-, 1-, 2-, and 3-hour periods. Clear trends between pretreatment conditions and BSG recovery and its subsequent maximal solubility (in the following step of our overall process to produce microbeads) were observed during our investigation and are illustrated in Table 1. These findings are in keeping with previous studies on the dilute acid hydrolysis of BSG.[57-60] First, our results demonstrate that the acidity of the solution has an important impact on pretreatment performance. When other parameters remain steady, our results show that higher acid concentration (0.45 *vs.* 0.23) reduces BSG recovery, but improves grain solubilization (Table 1, entries 1 *vs.* 4, 2 *vs.* 5, and 3 *vs.* 6).

The effect of temperature was equally studied. As is demonstrated in Table 1, for a given acid concentration, an increase in temperature from 75 to 90°C is accompanied by a significant decrease in BSG recovery without noticeable effects on solubility (Table 1, entry 5 *vs.* 7 and 6 *vs.* 8). In the context of the project, where the aim is to recover as much biomass as possible, temperatures over 90°C are not indicated.

As a result of these findings, we attempted to use a lower temperature of 50°C to optimize solubilization while minimizing loss. However, our findings showed that while this temperature elicited reduced loss, maximal solubility could not be achieved. Even when acid concentration increased to 0.6 M, the wt% of dissolved grain was inferior to that of all tests realized at 75°C (Table 1, entries 1–6 *vs.* 9–10).

Finally, our results demonstrate that the effect of pretreatment duration varies according to the other conditions. In some instances, maximum solubility was achieved after only 1 h (Table 1, entries 1 *vs.* 2 *vs.* 3, 7 *vs.* 8, and 9 *vs.* 10). In all other cases, this was attained after 2 h (Table 1, entry 5 *vs.* 6).

Overall, our experiments demonstrated that the mildest pretreatment conditions allowing for the maximal solubility of BSG in the following solubilization step were 0.45 M HCl (initial pH of BSG-dilute acid samples = 0.5; final pH = 1.2) for 2 h at 75°C (Table 1, entry 6). An increase in pH is to be expected throughout pretreatment, as the acid is partially consumed by the process.[60] BSG could equally be completely dissolved when pretreatment involved greater acid concentrations, longer periods, or higher temperatures, but BSG recovery generally decreased (Table 1, entries 6 *vs.* 7 and 7 *vs.* 8). Accordingly, the optimized conditions offer the best compromise between the recovery yield after pretreatment and achieving ensuing grain solubilization. At these conditions, the recovery yield was 52.5% after the overall pretreatment process (filtering and rinsing pretreated BSG to a neutral

TABLE 1 Brewer's spent grain (BSG) recovery after pretreatment and maximal pretreated BSG solubility during solubilization (Max. BSG) measured for different pretreatment conditions (select experimental data).

Entry	[HCl] (M)	Temp. (°C)	Duration (h)	BSG recovery (%)	Max. BSG (wt%, dry)
1	0.23	75	0.5	77	7.5
2	0.23	75	1	67	8
3	0.23	75	2	47	8
4	0.45	75	0.5	75	8
5	0.45	75	1	53	8.5
6	0.45	75	2	53	9
7	0.45	90	1	44	9
8	0.45	90	2	29	9
9	0.60	50	1	92	7
10	0.60	50	2	89	7

pH). Preliminary HPLC analysis of the filtrate confirmed that lignin degradation products, among other molecules, were removed from the BSG during pretreatment (Figure S1). A change in the visual aspect of BSG was also observed after pretreatment (Figure S2).

2.1.3 | Dissolution of brewer's spent grain

Our goal was to evaluate BSG's solubility in an eco-friendly, non-derivatizing aqueous NaOH system. This system's long-known compatibility with purified cellulose at specific cellulose and NaOH concentrations (7–8 wt% each) and low temperatures (around 5 to −10°C) provided a starting point for our work with pretreated BSG.[45] ZnO was identified as a potential additive to prevent the spontaneous gelation of the BSG solutions. The additive is also known to confer porosity to the final beads that may otherwise be hindered by the presence of residual lignin.[41,46] All tests of BSG solubility were evaluated after 24, 48, and 72 h.

A first series of samples (5 to 10 wt% BSG, 5 M NaOH, 1 wt% ZnO) were evaluated at 5°C. A second series of samples of the same composition were evaluated at 0°C and showed improved solubility (Figure S3). At −5°C, BSG solubility decreased. Given those results, the temperature was varied at 1°C increments between −5 and 0°C, which revealed optimal BSG solubilization at −2°C.

NaOH concentration was subsequently evaluated. All samples were prepared with 5 to 10 wt% BSG and 1 wt% ZnO and dissolved at −2°C. Sets of samples were prepared with 2.5, 10, and 15 M NaOH. An overall decrease in BSG dissolution was observed for the two more basic media (10 and 15 M) compared with our previous assays with 5 M NaOH. Conversely, samples prepared with 2.5 M NaOH were markedly more homogeneous than all our previous assays. Concentrations of 1, 1.5, 2, and 3 M NaOH were consequently evaluated. The best results were obtained at 2 M NaOH. The optimal temperature and NaOH concentration we determined for the dissolution of BSG are consistent with those of purified cellulose dissolved in NaOH-water systems.[45,61]

As a next step, ZnO concentration was evaluated. Sets of samples were prepared with either 0.5, 1, or 1.5 wt% ZnO. Our results showed that a minimum of 1 wt% ZnO was deemed necessary for the complete solubilization of up to 9 wt% BSG. This observation was surprising when considering the previous studies done on the solubilization of pure cellulose[62,63] in which ZnO is described as an additive that does not directly intervene in the cellulose solubilization mechanism, but rather prevents the spontaneous gelation of solubilized polysaccharides. Moreover, these studies also stated that above 0.5 wt%, the additive reportedly has no further desirable effects and precipitates, contrasting what we observed with our more complex matrix.

Although our first series of experiments led us to develop an efficient system that allowed complete BSG solubilization up to 9 wt%, all our attempts to generate microbeads (in the following stage of our overall process) from those solutions failed. The addition of pure cellulose to these solutions allowed us to circumvent this limitation and obtain microbeads following the solubilization step. To study this parameter, various quantities of different types of purified cellulose were added to samples consisting of 9 wt% BSG dissolved in 2 M NaOH with 1 wt% ZnO at −2°C over 24 h. Purified cellulose was not added from the beginning as it impeded BSG solubility and increased solubilization time. In short, our different assays showed that the degree of polymerization (DP) of the purified cellulose used directly influenced the required time to solubilize the additive, as well as the quantity needed to obtain quality microbeads.

Specifically, cellulose chains with greater DP took more time to dissolve, but successful microbead regeneration required less long-DP cellulose than short-DP cellulose. These observations are consistent with previously reported thermodynamic and rheometric data on cellulose fiber solubilization.[45,64,65] Our experiments showed that medium DP fibers (Celova® 500, alpha-cellulose fiber, or cellulose fiber medium) offered the best compromise between fiber DP and solubilization time. Incorporating 2 wt% of medium DP cellulose into the BSG solution, followed by an additional 24 h of stirring, allowed us to obtain solid, resistant microbeads at the end of the process. The beads characterized throughout this manuscript were prepared with alpha-cellulose fiber.

2.1.4 | Shaping and solidification of brewer's spent grain beads

A 1 mL syringe was used to withdraw and extrude sample solutions, one drop at a time, into a tenfold (*v*/*v*) acidic or saline solution. The solid beads could then be recuperated by filtration over a Büchner funnel (1 mm pore size). The humid microbeads obtained were oven-dried to yield the final BSG bead product.

Various aqueous coagulation media were tested to generate the beads (Figure S4). Solutions of HNO_3, no matter their molarity, provided poor results. Beads yellowed, suggesting the oxidative effect of HNO_3. Saline solutions of 10 wt% NaCl inconsistently solidified the beads; generally, beads demonstrated weak mechanical properties. Greater concentrations of the saline solution impeded bead solidification. Salt hydrates may penetrate

the beads and rupture hydrogen bonds between the cellulose fibers, impeding consistent solidification.[66,67] Our best results were obtained using aqueous HCl (from 0.5 to 4 M, at 0.5 M intervals) as our coagulation medium. These observations echo previously reported observations for the solidification of pure cellulose and hybrid cellulose-lignin microbeads.[42,46,68] Although all the tested concentrations of HCl lead us to generate satisfactory microbeads, at 1 M HCl the beads were removed from the acid bath with minimal observed breakage.

The size of the needle used for dropping the BSG solution in the coagulation bath directly influenced the size of the resulting beads, with smaller needle diameters yielding smaller beads (Figure 2 and Table 2). However, the two parameters are imperfectly correlated as illustrated in Table 2 (i.e., by reducing needle ID by approximately 50%, bead diameter only reduces by approximately 5%, with surface tension as the likely limiting factor).[69] Microbead shaping was achieved using needles with IDs greater than 260 μm. Needles with smaller IDs were assessed but could not be used for dropping due to the high viscosity of the BSG solution (approximately 6000 cP).

The optimal drop height was between 1 and 2 cm. At greater heights, the beads flattened upon impact; lesser heights did not allow sufficient droplet breakup but showed promise for extending the dropping technique to jet-cutting to achieve even smaller bead dimensions.[40] The same size beaker and the same volume of solution were used for each test so that variations in surface tension could be directly attributed to the inherent nature of the solutions.

Ambient temperatures yielded the best results. At higher temperatures, the beads dissolved into the coagulating solution; at lower temperatures, the beads seemed to solidify but did not hold up to filtration. Longer contact periods between the newly formed beads and the coagulation solution provided the best solidification of beads. Periods of regeneration shorter than 12 h provided beads of reduced mechanical properties.

2.1.5 | Overall optimized process outcome

Our optimization work on the different steps (pretreatment, dissolution, and solidification) led us to develop an overall process to convert raw humid BSG into solid microbeads with an evaluated overall yield of 31% (dry weight basis). First, dilute acid hydrolysis pretreatment (0.45 M HCl, 2 h, 75°C) allowed to recover 53% (dry weight basis) of BSG as a pretreated (easier to solubilize) biomass. This pretreated grain (9 wt% BSG) was then solubilized in a 2 M NaOH solution at −2°C, alongside 1 wt% ZnO, over 24 h. Then, 2 wt% medium DP cellulose

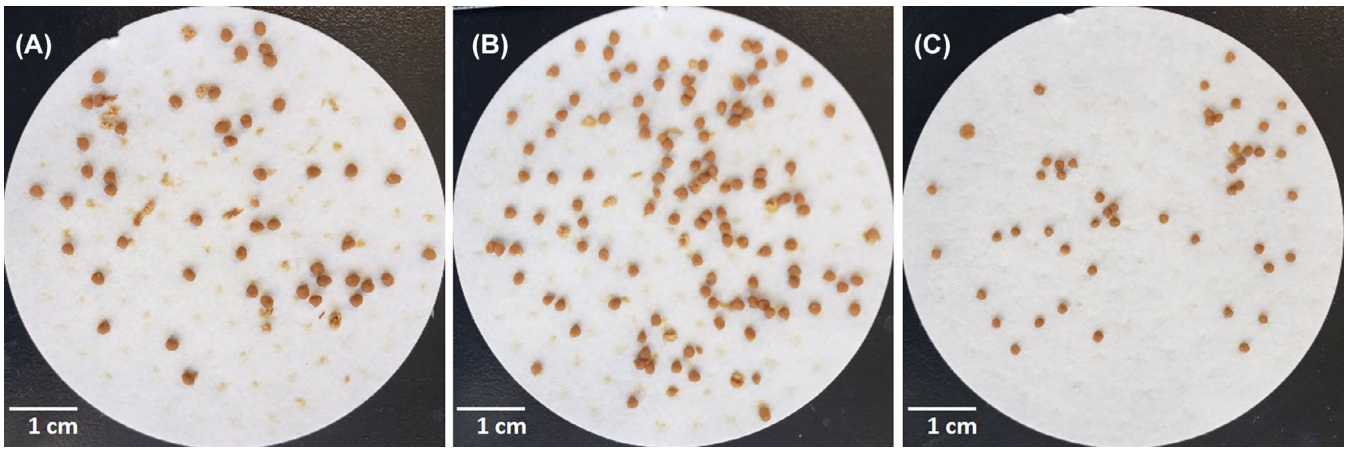

FIGURE 2 Images of humid microbeads prepared from brewer's spent grain solutions extruded through syringes using various needle sizes: (A) 21 G, (B) 22 G, and (C) 26 G.

TABLE 2 Microbead dimensions and characteristics as a function of needle size ($n = 90$).[a]

Needle gauge (G)	Needle ID (μm)	Feret's diameter (mm)	Weight (mg)	Roundness
21	514	1.31 ± 0.20	1.25 ± 0.12	0.71 ± 0.11
26	260	1.25 ± 0.20	0.94 ± 0.12	0.86 ± 0.10

[a]Beads obtained from a 22 G needle (and displayed in Figure 2B) were not characterized to the same extent as 26 G and 21 G beads and are thus omitted from the table.

fibers (alpha-cellulose fibers) were added to the solution and were solubilized over a further 24 h. The resulting homogeneous solution could then be extruded through a syringe equipped with a 26 G needle (other needles with IDs greater than 260 μm can equally be used) from a 2 cm drop height into a 1 M HCl solution. Microbeads were left to solidify in this solution for 12 h at ambient temperatures; they were then carefully filtered from the solution, dried, and set aside for further characterization. Considering the resulting mass of dried microbeads and assuming that microbeads contain the same proportions of BSG and purified cellulose as the solution (9:2 ratio), the yield of the solubilization/solidification sequence can be evaluated at 58% (dry weight basis). With the current processing conditions, this corresponds to an E-factor of 130 (see the Supporting Information). It is important to note that 43 points of the E-factor correspond to the acid filtrate from pretreatment that can be reused at least twice, and 73 points correspond to the acid filtrate from bead shaping that can be reused at least 6 times.

Reducing BSG-solution losses during microbead shaping and solidification could improve the yield and reduce the E-factor of the overall process. Indeed, during our experiments, the BSG solution could not be recovered in its entirety from the equipment used for its solubilization (Erlenmeyer flask and magnetic stirring bar), nor from the exterior of the needle and syringe used for microbead shaping. Those issues are currently being addressed as we are working on scaling up our process.

As evoked above, to improve our process's sustainability and reduce the loss of other solutions involved in BSG-microbead production, we tested the reutilization of the pretreatment medium and the coagulation solution for multiple bead production cycles. The 0.45 M HCl solution used for pretreatment can be used at least twice, provided the pH is adjusted back to initial levels. As for the 1 M HCl coagulation solution, the same solution can regenerate six batches of beads as long as the tenfold ratio between BSG solution and acid (*v*/*v*) is respected throughout. We also experienced that after these six cycles, the used coagulation solution can be repurposed, after pH adjustment, as a medium for the pretreatment step, with no negative effects on the overall process and improving the process' E-factor.

2.2 | Characterization

2.2.1 | Raw brewer's spent grain composition

The batches of brewer's spent grain used throughout this project to verify the method's reproducibility were analyzed by a unique combination of NREL, ASTM, and TAPPI protocols[70] as well as the Kjeldahl method[71] to determine their molecular composition. Results presented in Figure 3 shows low variability in terms of the molecular composition from four batches. Results are normalized and expressed in terms of percent composition, where the total of the fractions for each sample adds up to 100. Complete biomass composition data, as well as biomass appearance throughout the process, can be found in the Supporting Information (Table S1 and Figure S3).

Extractives (i.e., volatile organic compounds, monomeric sugars, and degradation products) represent the largest component of each sample at an average of 30.9%. Previous studies on the composition of BSG present these as a much less significant fraction of the biomass, accounting for around 10% of samples.[54] Higher extractive content thus diminishes the relative proportions of all other components in our samples. Yet: ash, protein, and total lignin content fall within the expected ranges, and average cellulose and hemicellulose content are respectively 2.9% and 4.2% lower than anticipated.

As cellulose is the main component of interest in BSG for the intended application, proving the method's suitability for relatively low cellulose content can be interpreted as a positive. Previous studies place cellulose content in BSG between 2.9% and 12.1% higher than our reported average of 14.1%.[54,72]

Discrepancies between our results and those found in the literature, notably about extractive content, are likely due to differences in analytical protocols. Values presented in the literature are the result of one or two-cycle Soxhlet extractions,[52,55] while values presented here are the result of a four-cycle Soxhlet extraction (hexane, toluene-ethanol, ethanol, and water) which provides more comprehensive extractive quantification.[70] Humidity content is consistent with the literature: the average humidity of our samples (77%) is the lower bracket of the previously reported range (77%–85%).[54,55]

2.2.2 | Brewer's spent grain composition after pretreatment

The BSG's molecular composition changes as a result of pretreatment (dilute acid hydrolysis, filtration, rinsing). Figure 3B shows how the composition of raw BSG (Batch 1) differs following this step (see Table S1 for complete data). Regarding our desired application, we can affirm that pretreatment effectively fractionated the BSG as it enriches the sample in alpha-cellulose and lignin by removing extractives, acid-soluble lignin, and proteins. Although higher acid concentration (0.45

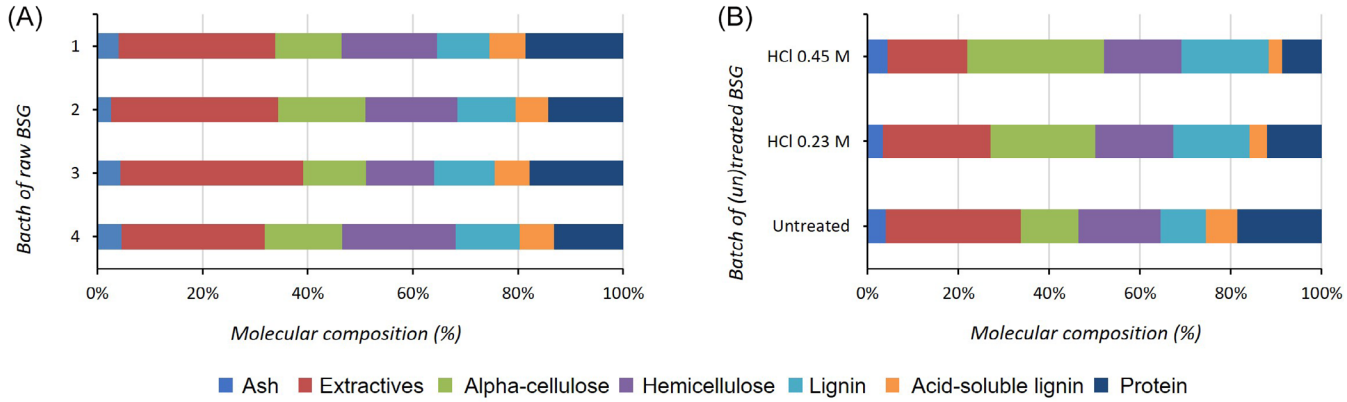

FIGURE 3 Molecular composition of (A) different batches (Batch 1–Batch 4) of raw brewer's spent grain and (B) a unique batch of brewer's spent grain following pretreatment for 2 h at 75°C in either 0.23 or 0.45 M HCl.

vs. 0.23 M) leads to only slightly lower recovery yields in pretreated pulp (Table 1, entries 3 *vs.* 6), the pulp is significantly enriched in alpha-cellulose and more readily dissolved in aqueous NaOH-ZnO. These observations support previous works that suggest that protein needs to be extracted from lignocellulosic biomass before carbohydrate content can be dissolved.[73] The mechanism is likely synergistic: by extracting protein and enriching the sample in cellulose and lignin—for which the NaOH system has already proven to be compatible—BSG can be effectively solubilized after pretreatment using a lower acid concentration.[46]

Using the optimal pretreatment conditions for our overall process (0.45 M HCl, 2 h, 75°C), the resulting pretreated BSG ends up with a combined composition of 69.3% of cellulose, hemicellulose, and lignin (including acid-soluble lignin). As 9 wt% of this pretreated biomass can be dissolved alongside 2 wt% cellulose during the solubilization step, this brings the total content in cellulose, hemicellulose, and lignin to just above 8 wt% (6.2 wt% from pretreated BSG + 2 wt% purified cellulose in samples). Interestingly, pure cellulose solubilization is restricted to a maximum of 8 wt% solids for 2 M NaOH with ZnO as an additive.[63] Hybrid cellulose-lignin beads, reported by Gabov et al.[46] do not surpass 5 wt% cellulose and 3.4 wt% lignin for similar conditions. Our findings demonstrate that we can dissolve a greater quantity of total solids (9 wt% BSG + 2 wt% cellulose) but similar amounts of cellulose, hemicellulose, and lignin (with respective totals of 4.7, 1.5, and 2.0 wt% of these compounds in the samples). These observations indicate that, although pretreatment is a necessary step, residual protein and extractives in pretreated BSG do not impede lignocellulosic fiber solubilization and may boost total solids content in the final product.

2.2.3 | Weight, size, and shape of dried microbeads

Bead weight, size, and shape were influenced by the interior diameter of the needle used for their production. For a 21 G needle (ID = 514 μm), the microbeads ($n = 91$) had an average Feret's diameter of 1.31 ± 0.20 mm, a weight of 1.25 ± 0.12 mg, and a roundness of 0.70 ± 0.11. A 26 G needle (ID = 260 μm) provided the closest possible dimensions to current industry standards (shower gels, mean diameter of 419 μm; facial cleansers, mean diameter of 197 μm) while using the dropping/extrusion method.[74] Indeed these beads had a Feret's diameter of 1.25 ± 0.20 mm, a weight of 0.94 ± 0.12 mg, and a roundness of 0.86 ± 0.10. This information is compiled in Table 2. The envisioned automation of the dropping technique through jet-cutting is likely to reduce bead size, resulting in a similar microbead Feret's diameter to that of the ID of the extruding needle.[40] This hypothesis was tested by measuring the diameter of filaments produced by the continuous extrusion of our BSG solution into the acid bath. We were pleased to observe that when using a 26 G for the continuous extrusion, we obtained filaments with an average Feret's diameter of 0.34 mm after drying (see Figure S5).

2.2.4 | Swelling of dried microbeads in water

The total area occupied by a sample of 20 microbeads (extruded from a 26 G needle) before and after their soaking in room temperature water for 24 h was compared by taking pictures and treating them using ImageJ software. Assuming perfect bead sphericity, the area can be used as an indicator of changes in total bead volume. Wet beads were 17% larger than dried beads, indicating the

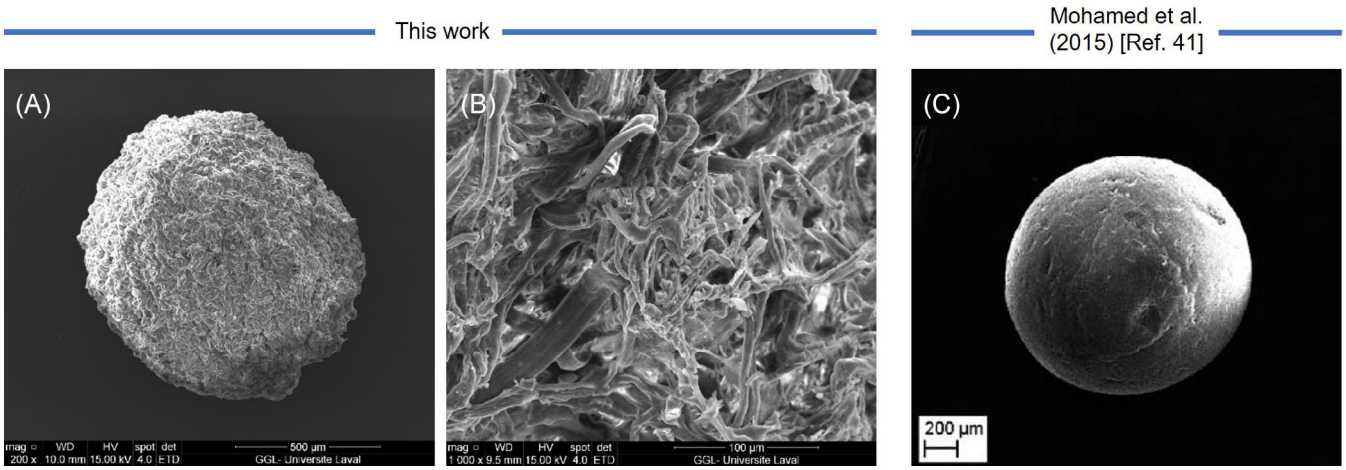

FIGURE 4 Scanning electron microscopy images. Brewer's spent grain microbead extruded using a 26 G needle: (A) exterior at 200× magnification, (B) interior cross-section at 1000× magnification. (C) Example of a cellulose microbead fabricated using a similar NaOH system (Reproduced from Ref. 41 with permission from the Royal Society of Chemistry).

permeability of their outer layer and their porous interior structure. This is consistent with information regarding hybrid cellulose-lignin microbeads from purified natural polymers, which exhibit 15%–20% swelling for similar wt % cellulose and lignin.[46]

2.2.5 | SEM-EDS

Scanning electron microscopy (SEM) revealed the microbeads' exterior and interior morphologies (microbeads prepared using a 26 G needle; Figure 4A,B). At 200× magnification, beads' surfaces do not have sharp edges (which are characteristic of naturally hard materials ground into exfoliating particles),[23,24,75] and fibers are densely intertwined. The presence or absence of pores can be determined from this picture (Figure 4A). Average roundness was evaluated at 0.61 for our smallest microbeads (average diameter of 1.25 mm) after measuring three separate particles at this magnification. Cross-section images reveal a less dense interior structure with a greater number of visible pores (Figure 4B). When compared with purified cellulose microbeads (Figure 4C) prepared in a similar NaOH-ZnO-based system according to Mohamed et al.,[41] BSG microbeads appear to have increased porosity, yet reduced sphericity and smoothness.

Energy-dispersive spectroscopy (EDS) provided insight into the microbeads' elemental composition (Table 3). Semi-quantitative analysis ($n = 3$) revealed an average of 54.22 wt% C, 39.61 wt% O, 0.63 wt% N, and 1.32 wt% Si at the microbeads' surface layer. The interior layers of the beads did not significantly differ, with mainly 54.20 wt% C, 40.71 wt% O, 0.97 wt% N, and 1.48 wt% Si. Trace amounts of Al, Cl, Cu, and Zn were detected throughout the beads, which may be attributed to the elemental composition of BSG,[76,77] or residual HCl in the case of detected Cl (Table 3). In the case of Zn, it is most likely that these trace amounts are due to residual ZnO trapped within the beads. However, this indicates efficient solvent/anti-solvent diffusion between the microbeads and the solidification bath, as Zn would otherwise be present in much higher amounts. This is consistent with the findings of Mohamed et al.,[41] who produced microbeads from an aqueous cellulose-NaOH-ZnO solution using the dropping technique and found that acid-regenerated beads did not contain ZnO. Sodium is not detected, indicating that the beads were completely neutralized in the acid bath and thoroughly rinsed, further proving efficient anti-solvent polymer regeneration.

2.2.6 | ATR-FTIR

Spectroscopic analysis of dried BSG microbeads (average diameter of 1.25 mm) provided insight into their composition in comparison with the added purified cellulose powder (alpha-cellulose fibers, Sigma Aldrich) and raw BSG used in their production (Figure 5). The broad absorbance bands around 3300 cm^{-1} for both starting materials and the final beads corresponds to the stretching vibrations of O—H and N—H groups.[78] For purified cellulose and the microbeads, this absorbance band is centered at a higher wavelength, likely due to the greater influence of the O—H bonds. Moreover, this absorbance band is broader for microbeads than for purified cellulose, suggesting enhanced intermolecular hydrogen bonding in the final product.[41,79] A sharper absorbance band around 2850–2950 cm^{-1} can be attributed to C—H

TABLE 3 Average ($n = 3$) elemental composition (wt%) of brewer's spent grain microbeads as determined by energy-dispersive spectroscopy.

Element	C	N	O	Al	Si	Cl	Cu	Zn
Exterior	54.22 ± 0.51	0.63 ± 0.89	39.61 ± 1.26	0.04 ± 0.04	1.32 ± 0.20	0.72 ± 0.12	1.93 ± 0.90	1.51 ± 0.75
Interior	54.20 ± 0.31	0.97 ± 0.72	40.71 ± 1.04	0.07 ± 0.05	1.48 ± 0.27	0.56 ± 0.10	0.94 ± 0.78	0.67 ± 0.15

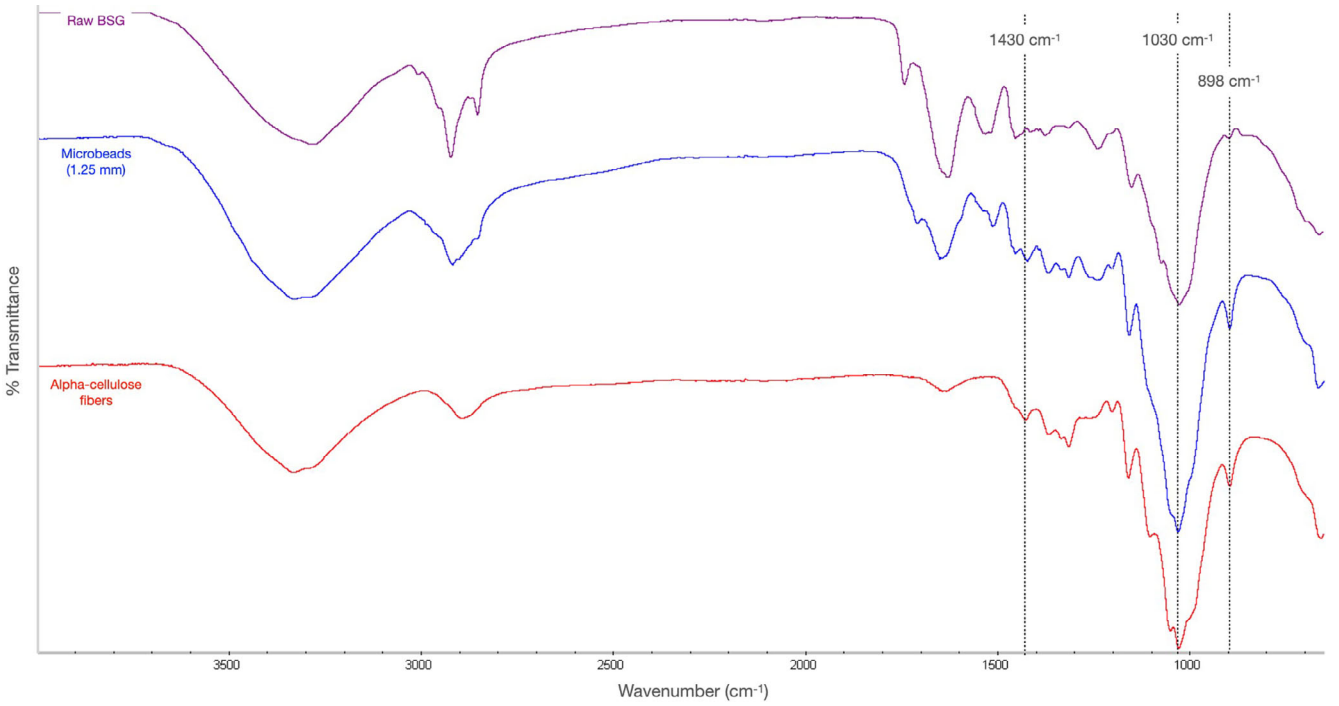

FIGURE 5 Fourier transform infrared spectra for raw brewer's spent grain (BSG) (purple), BSG-based microbeads (1.25 mm diameter, blue), and alpha-cellulose fibers (red).

bonds and is most intense for BSG due to the biomass's greater molecular complexity.[80] A small absorbance band centered around 1430 cm^{-1} is characteristic of the crystal region of cellulose I.[41] It is strongest in the purified cellulose sample and persists in the microbeads, indicating that cellulose I is not completely lost during the solubilization-regeneration process. Another intense band is observed around 1620–1660 cm^{-1}, especially for BSG. As absorbance bands in this area are most often associated with aromatic skeletal vibrations (C═C) and the carbonyl stretch (C═O) of ketone and carboxylic acid groups,[80,81] unsurprisingly, absorbance bands are most intense for raw BSG, then for microbeads, and relatively weak for purified cellulose (the absorbance band at 1634 cm^{-1} for alpha-cellulose is attributed to absorbed water).[82,83] In the range of 1100 to 1500 cm^{-1}, a greater number of absorbance bands for BSG and microbeads' spectra further demonstrate their greater molecular complexity over purified cellulose, notably with N—H and C—N deformations.[84] In all three spectra, an intense absorbance band is observed around 1030 cm^{-1}, which can be associated with the C—O—C pyranose ring vibration known to be integral to the samples.[85] As for the absorbance band around 898 cm^{-1}, this represents the ß-glycosidic linkages of cellulose,[85] hence its relative weakness in raw BSG. This absorbance band is sharper and more intense for the microbeads than in the case of purified alpha-cellulose, indicating increased intermolecular hydrogen bonding in the final product.[41,79]

Overall, the comparison of microbeads' spectra with those of their precursors once again confirms that beads are not solely composed of cellulose. Instead, absorbance bands observed in the IR spectra of microbeads mirror those found in the spectra of purified cellulose and raw BSG, showing that the final product does indeed result from the solubilization and regeneration of both. Slight shifts in the absorbance bands' maxima are indicative of this solubilization-regeneration process and the appearance of cellulose II. Despite an increase in intermolecular hydrogen bonds in the final product, cellulose also partially remains as cellulose I, as evidenced by the absorbance band around 1430 cm^{-1}. Both allomorphs of cellulose indicated in the final product (cellulose I and II) are readily biodegradable.[86]

2.2.7 | Microbead hardness

Some of the microbeads' key mechanical properties (for the smallest beads, at an average 1.25 mm diameter) were determined by microindentation testing. From this, the average ($n = 15$). Indentation modulus (M) and hardness (H) values were found to be 5.64 ± 1.04 GPa and 199.05 ± 43.80 MPa, respectively. The coefficient of variation (CoV) for M and H values are 18.4% and 21.0%, respectively, at the maximum penetration depths (h_{max}) of continuous multi-cycle (CMC) micro-indentation tests. The average value and CoV seem to converge at a constant value after 10 tests, representing that the uncertainty cannot be reduced by further testing. Instead, uncertainty is a consequence of the material microstructure. Complete CMC results can be found in the Supporting Information (Table S2).

Average bead hardness (H) is the key piece of information resulting from microindentation testing. It is important to ensure that microbeads in personal hygiene products are hard enough to remove contaminants from the skin without damaging human tissues. Polymers used for microbeads are generally between 22 (low-density polyethylene) and 245 MPa (polyacrylic acid) with the exact hardness as a function of the specific polymer.[87] Current common alternatives to plastic microbeads generally use harder materials. Apricot pit hardness is around 244 MPa,[88] various natural nutshells (i.e., coconut and walnut shells) cover a range of 290 to 570 MPa,[89,90] and sodium tetraborate crystals present a hardness of 417 MPa.[88] The greater hardness of these materials, in addition to their jagged, irregular particle shape, represents a greater likelihood of damaging the skin. Recently, another study reported that chitin-based microbeads with a hardness of 113–128 MPa can be used as potent exfoliating agents, while samples with a hardness value of 83 MPa could not.[22] In comparison with these values, BSG microbeads with a hardness value of 199 MPa meet the industry standard required for vigorous and non-damaging exfoliating microbeads.

2.2.8 | Stability in matrices relevant to personal hygiene products

Our BSG microbeads' stability was evaluated over a month in various matrices: water, two commercial shower gels, and a commercial body cream. BSG microbeads proved to be incompatible with the body cream matrix (complete disintegration, likely due to the relative hydrophobicity of the body cream) and could not be separated from the cream for further characterization.

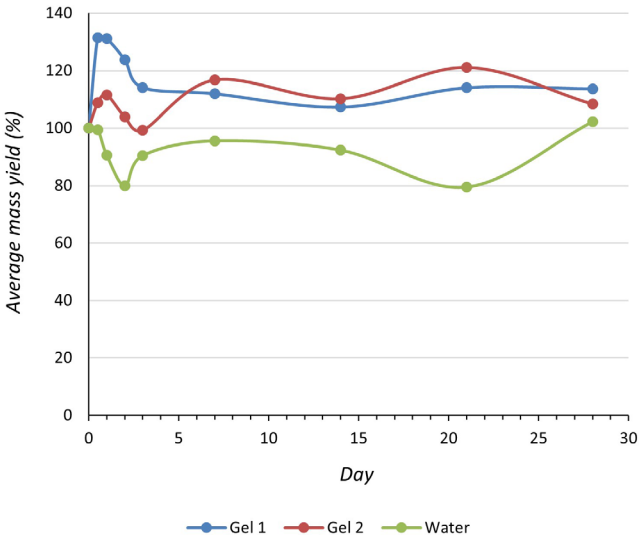

FIGURE 6 Graphical representation of the average mass yield for brewer's spent grain microbeads (average diameter = 1.25 mm) aged in shower gels (Gel 1, Gel 2) and water over a month-long period.

In both body washes and water, beads maintained their solid structure for all samples. Figure 6 demonstrates the beads' stabilities in terms of average mass yield (%). Beads incorporated into shower gel samples (Gel 1 and Gel 2) had average mass yields above 100% except for Gel 2, day 3, at 99%). This may be due to the beads' absorption of surfactants or other chemical species able to penetrate the beads' fibrous structure from the shower gels. In Gel 1, the average bead mass yield was highest over the first few days, then seemed to stabilize around 110%. In Gel 2, the average bead mass yield slowly and inconsistently rose over the 28 days, seemingly stabilizing around 110% as well. Beads incorporated into water presented their lowest mass yield after 21 days (80%) and their highest mass yield after 28 days (102%), while demonstrating the least variability among replicates. This final mass yield may be due to residual water, trapped within the beads, or to the formation of an imperceptible biofilm. In general, bead mass yield hovers around 90% in water. Complete stability data for these assays can be found in the Supporting Information (Table S3).

BSG microbeads of two different sizes (average diameter of 1.25 and 1.31 mm, or 26 and 21 G, respectively) were incorporated in a solid glycerin soap base and evaluated. Solid soap samples containing roughly 3 wt% of BSG microbeads were conserved under ambient conditions and qualitatively monitored for their stability over 3 months. For both sizes of beads, samples did not exhibit any signs of decomposition: bead integrity and macroscopic mechanical properties remained stable throughout the experiment period. Concomitantly, samples of

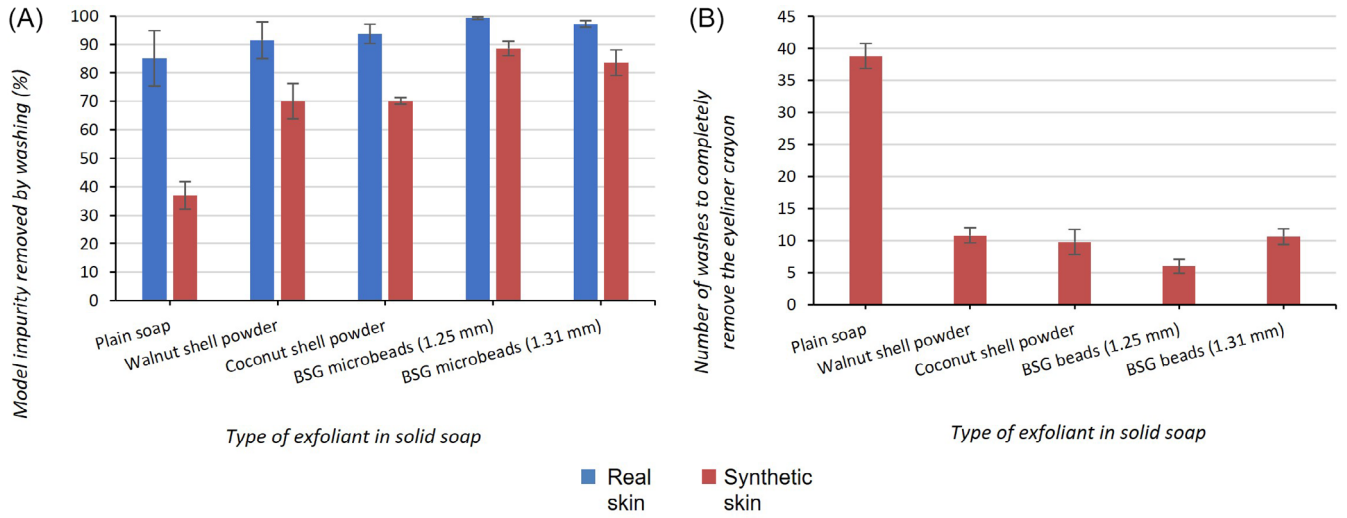

FIGURE 7 (A) Evaluation of various soaps' capacities to remove a model impurity from real and synthetic skin; (B) representation of the number of washes required to completely remove a model impurity from synthetic skin.

microbeads (both sizes) were separately conserved under ambient conditions and monitored for stability over a year. Neither sample exhibited signs of decomposition or other physical or chemical alterations throughout this period.

2.2.9 | Cleansing efficiency

Solid soaps containing roughly 3 wt% of natural exfoliating particles (ground walnut or coconut shells) were compared with soaps containing different sizes of BSG microbeads (average diameter of 1.25 and 1.31 mm, or 26 and 21 G, respectively) and a control (plain soap) in terms of their ability to remove eyeliner pencil from real skin and synthetic skin after a standard number of washes. Figure 7A shows that all soaps containing exfoliating particles performed better than the control, validating that physical exfoliating agents help remove dirt from the skin and encourage epidermal desquamation.[23,25] Exfoliating soaps were more effective on natural skin than on synthetic skin, although replicates demonstrated a greater degree of error. The smallest BSG microbeads (1.25 mm diameter, 26 G) demonstrated the best performance, likely due to the larger specific surface area of smaller beads.[22,74] Figure 8 demonstrates a series of photos offering a visual demonstration of the cleansing efficiency of those microbeads, compared with plain soap or soap containing natural exfoliating particles (coconut shell powder).

Soaps were equally evaluated for the number of washes it took to completely remove an eyeliner pencil mark from synthetic skin (Figure 7B). All soaps containing physical exfoliating agents demonstrate superior cleansing capacities than the control, which required an average of 38.8 washes. Larger BSG microbeads have a comparable cleansing efficiency to the other commercially available natural exfoliating agents (10.6 washes compared with 10.8 and 9.8 washes for walnut and coconut, respectively). When coupled with the data from the previous cleansing efficiency testing (Figure 7A), this represents that soaps containing larger BSG-beads may be more effective than commercial exfoliating agents over the first five washes, but that they converge to similar efficacy after nine to ten washes. However, the smallest BSG microbeads demonstrate the greatest cleansing efficiency of all exfoliating agents with an average of six washes required to completely remove the crayon. This indicates that exfoliation with soaps containing small BSG microbeads may reduce cutaneous irritation associated with physical exfoliating agents that require a greater number of washes to achieve similar cleansing efficiency.[23,25]

3 | CONCLUSION

Brewer's spent grain was shown herein to be a promising starting material in the development of exfoliating microbeads. After dilute acid hydrolysis, pretreated BSG could be dissolved up to 9 wt% (solids basis) in 2 M NaOH with 1 wt% ZnO as an additive. BSG solubilization occurred at −2°C over 24 h, with an additional 24 h to dissolve 2 wt% alpha-cellulose powder. Spherical beads were produced by extruding the BSG solution through a syringe into a 1 M HCl coagulation solution. When

FIGURE 8 Visual representation of the removal (with the same washing procedure) of a model impurity on the skin by (A) plain soap, (B) soap containing brewer's spent grain beads with an average diameter of 1.25 mm, and (C) soap containing a commercial natural exfoliant (coconut shell powder). Before photos are on the left and after photos are on the right.

a 26 G syringe was used, the microbeads obtained after filtration and drying had an average diameter of 1.25 mm. Assuming that microbeads contain the same proportions of BSG and purified cellulose as the solution, our process allows us to transform 31% of raw BSG into microbeads (dry weight basis). BSG microbeads exhibit porous internal structures, as suggested by their swelling in water and as confirmed by SEM imaging. Beads do not contain residual NaOH and only trace amounts of ZnO, and FTIR indicates the presence of cellulose I and II, attesting to the biodegradability of the material.[86] Although long-term stability testing will eventually be necessary for the commercialization of BSG microbeads, we noted that they exhibited promising stability in commercial shower gels and distilled water over a month-long observation period. Otherwise, BSG microbeads did not exhibit any signs of physical or chemical alteration in solid soaps over 3 months, nor under ambient, dry conditions over 1 year. Moreover, the BSG microbeads exhibit improved cleansing abilities when compared with commercially available natural exfoliating particles, while offering a less skin-damaging hardness of 199 MPa. In sum, BSG microbeads are a promising option for exfoliating particles in personal hygiene products and provide a high-value application for abundant residual biomass. We are currently working on scaling up our overall process to treat higher volumes of biomass and reduce losses during the transfer of the coagulation solution. The production of smaller microbeads by an automated method (i.e., the jet-cutting technique in place of dropping/extrusion) will also be investigated.

4 | EXPERIMENTAL

4.1 | Materials

4.1.1 | Brewer's spent grain

Brewer's spent grain (BSG) was obtained from two local Quebec microbreweries throughout this project: Le Bien le Malt (Rimouski, QC, Canada), and Ras L'Bock (La Pocatière, QC, Canada). We worked with four batches of BSG obtained from different brews to account for the effects brewing conditions may have on BSG's composition. The exact cereal composition of these samples was never specified, but the main component was always malted barley. Samples had an average humidity of 77%, as determined gravimetrically.

4.1.2 | Other materials

Purified cellulose fibers were obtained from various sources. Celova® Cellulose Powder samples (C500, C1000, and C2000) were provided by Weidmann Fiber Technology (Switzerland). Microcrystalline cellulose was purchased from Alfa Aesar (USA). Cellulose fibers (medium) and alpha-cellulose fiber (99.5%) were purchased from Sigma-Aldrich (USA). See Supporting Information for product specifications about cellulose fiber length (Table S4). Non-nano zinc oxide (approx. 200 mesh powder, 99.9%) and sodium hydroxide pellets (98%) were obtained from Alfa Aesar (USA). Hydrochloric acid

(ACS grade, 36.5%–38%) and nitric acid (ACS grade, 68%–70%) were purchased from VWR (USA).

4.2 | Preparation of brewer's spent grain microbeads (typical optimized procedure for 50 g of BSG solution)

Humid BSG was first pretreated by dilute acid hydrolysis with HCl. Accordingly, 77% humidity BSG was combined with dilute acid at a 1:4 mass ratio (37 g of humid BSG and 148 g of dilute acid, 0.45 M HCl) and heated at 75°C for 2 h. The pretreated solid was then filtered using a 1 mm sieve to separate it from the liquid hydrolysate, and washed with distilled water until the pH of the rinsing solution was neutral. A yield of 53% of BSG (dry) was measured for this step. Pretreated BSG (9 wt%, dry basis, corresponding to 4.5 g of dry BSG solids) was then transferred to a 125 mL Erlenmeyer equipped with a magnetic stir bar. An aqueous solution of 2 M NaOH was added, alongside 1 wt% ZnO. The solution was stirred for 24 h at −2°C (a recirculating chilling bath was used to maintain the temperature). After 24 h, 2 wt% medium-DP cellulose fibers [Celova® 500, Weidmann Fiber Technologies, Switzerland; cellulose fibers (medium) or alpha-cellulose fibers, Sigma-Aldrich, USA] were added and the mixture was stirred for an additional 24 h. The total sample weight was 50 g. From the resulting BSG solution, the shaping of the beads and the regeneration of the polymeric structure were completed using the dropping/extrusion technique. The BSG-NaOH-ZnO solution was introduced, drop by drop, into a tenfold (*v/v*) acidic regenerating solution (1 M HCl, ambient temperature), at a drop height of 2 cm (in 250 mL beakers). The BSG solution was extruded through a 1 mL syringe equipped with a 26 G needle. Depending on the desired size of microbeads, various needle sizes can be used during the extrusion step (Table 2), the smallest compatible needle size being 26 G. After 12 h, the resulting beads were filtered from the regeneration solution and dried in an oven at 50°C, yielding a total of 3.2 g of dry BSG beads from the 50 g of BSG solution prepared. The beads were stored in a closed vessel at ambient temperature for later characterization.

Assuming that dry microbeads contain the same proportions of BSG and purified cellulose as are in the BSG solution samples (4.5 g of BSG and 1 g of purified cellulose, dry weights), this 3.2 g of dry BSG beads should contain 82% BSG (BSG beads only contain BSG and cellulose, confirmed by EDS). Consequently, 2.6 g of this mass of dry BSG beads can be attributed to BSG, and the global yield of BSG solids for the method is 31%.

4.3 | Characterization

4.3.1 | Brewer's spent grain humidity and composition

The humidity of the biomass was determined gravimetrically after drying the biomass at 100°C. After 16 h, samples were weighed ($n = 3$) and placed back in the oven for a further 4 h. Dry mass was determined once the sample's weight stabilized (less than ±5% variation in mass from the previous measurement); otherwise, samples were dried for further 4 h intervals until their mass was stable. Humidity was calculated according to Equation (1):

$$\text{Humidity}(\%) = \left[1 - \left(\frac{m_f}{m_i}\right)\right] \times 100 \quad (1)$$

where Humidity is the gravimetrically-determined humidity of the sample expressed in terms of %, m_f is the final dry, stable mass of the sample in grams, and m_i is the initial wet mass of the sample in grams.

Samples of 100 g of dry BSG—both as a raw material and after the various tested pretreatment methods—were analyzed for ash, extractives, alpha-cellulose, hemicellulose, lignin, and acid-soluble lignin. These components were quantified according to a combination of NREL, ASTM, and TAPPI protocols reported by Damay et al.[70] Briefly: a first extract is obtained after four successive Soxhlet extractions with hexane, ethanol/toluene (2:1, *v/v*), ethanol, and water. Then, the ash content is determined after heating the sample at 575°C. Holocellulose was isolated by depolymerizing and solubilizing lignin using acetic acid and sodium chlorite, then filtering on a fritted glass funnel. Alpha-cellulose is then isolated from holocellulose by treatment with sodium hydroxide and acetic acid, followed by filtration. Hemicellulose accounts for the remaining fraction, assuming holocellulose is solely composed of alpha-cellulose and hemicellulose. Lignin and acid-soluble lignin were quantified by hydrolysis with concentrated sulfuric acid, which allowed the separation of the different fractions of the biomass. Finally, protein content in BSG samples was quantified using the Kjeldahl method.[71]

4.3.2 | Weight, size, and shape of dried microbeads

The weights of individual beads were determined using a precision scale (Cubis®, Sartorius, Germany). Size and shape were determined by taking pictures of beads on a

clean, high-contrast surface. The images were then analyzed using ImageJ software (National Institutes of Health, USA). The size was represented as Feret's diameter, while the shape was represented in terms of roundness. Bead measurements were calculated according to Equation (2):

$$\text{Roundness} = 4 \times \frac{\text{area}}{\pi \times [\text{major axis}]^2} \quad (2)$$

where Roundness is the calculated roundness of the sample (a perfect circle has a value of 1.0), area is the surface area of the samples in mm^2, and major axis is the length of the line segment going through the farthest points on an ellipse in mm. A total of 90 beads were measured and averaged.

4.3.3 | Swelling of dried microbeads in water

The swelling behavior of air-dried BSG beads was determined by noting the changes in bead Feret's diameter by processing digital images using ImageJ software before (dry) and after soaking in distilled water at room temperature for 24 h (wet beads immediately after being filtered from the water). The swelling degree, expressed in %-units, was calculated as a function of the total surface area occupied by beads (determined by ImageJ), assuming perfect sphericity.

4.3.4 | SEM-EDS

The morphology of the regenerated, dried BSG microbeads was examined using an Inspect F50 (FEI Company, USA) scanning electron microscope (SEM). An energy-dispersive (EDS) detector (Octane Super-A, Edax Ametek, USA) was used to semi-quantitatively determine sample composition. Whole beads and their cross-sections (obtained by slicing beads with a razor blade) were coated with silver and palladium using a sputter coater. Three beads and cross-sections were imaged at 200× and 1000× at an optimum accelerating voltage of 15 kV, and their elemental composition was detected at a resolution of 131.7 eV.

4.3.5 | ATR-FTIR

Dried BSG microbeads (prepared from a 26 G needle), dry BSG, and purified cellulose (alpha-cellulose fibers, Sigma-Aldrich, used in the preparation of the beads characterized herein) were analyzed by ATR-FTIR using a Nicolet iS50 instrument (Thermo Scientific, USA). A total of 64 scans were realized for each sample at a resolution of 4 cm^{-1}. OMNIC spectra software (Thermo Scientific, USA) was used to normalize the spectra and investigate the absorbance bands.

4.3.6 | Sample hardness

Before microindentation testing to determine the microbeads' hardness, samples (1.25 mm BSG microbeads) were immobilized in epoxy resin discs. These discs were cured at 30% relative humidity and room temperature for a week. Discs were then sanded down (using 800 to 4000 grit sandpaper) and polished (using a velvet mat and 0–0.25 μm diamond polishing paste) to expose the interiors of the microbeads. Microindentation testing to determine sample hardness was performed with an ultra-high-resolution nano-indenter (UNHT, Anton Parr, Austria) equipped with real force and displacement sensors. This instrument virtually eliminates the effect of thermal drift and compliance due to its active surface referencing system and is consequently perfectly suited for long-term measurements of small-scale samples. The instrument was equipped with a Berkovich tip (at an indentation angle of 65.03°) and analysis was run according to the continuous multi-cycle method (CMC). Ten cycles were done with an acquisition rate of 30.0 Hz and a linear maximum loading increment. The first load was 1.00 mN, the maximum load was 30.00 mN, the time to maximum load was 2.0 s, the time to unload was 2.0 s, and unloaded to 30.00%. A 1.0-second pause was included between cycles. Before analysis, the instrument was calibrated with the samples to eliminate indentation offset, and preliminary CMC testing was carried out to determine the penetration depth at which the results can be considered homogeneous (unaffected by possible heterogeneity of the samples' microstructure). A total of 15 CMC tests were performed to measure the area of residual indentation in the sample by light microscopy (A_r) and the maximum load (P_{max}) in mN as a function of the penetration depth (h_{max}) in nm, as well as the unloading slope (S). The average maximum penetration depth (h_{max}) was 2767.96 ± 274.39 nm ($n = 15$). From these parameters, the sample hardness (H) in MPa can be calculated with Equation (3):

$$H = \frac{P_{max}}{A_r} \quad (3)$$

where H is the sample hardness (MPa), P_{max} is the maximum load (mN), and A_r is the residual indentation area (nm^2) as a function of h_{max}, the penetration depth (nm).

The indentation modulus (M) in GPa can also be calculated, according to Equation (4):

$$M = \frac{s \times \sqrt{\pi}}{2 \times \sqrt{A_r}} \quad (4)$$

where M is the sample indentation modulus (GPa), s is the unloading slope, and A_r is the residual indentation area (nm^2) as a function of h_{max}, the penetration depth (nm).

4.3.7 | Stability in matrices relevant to personal hygiene products

To measure the BSG microbeads' stability in model commercial personal hygiene products, 40 mg of beads (average diameter = 1.25 mm) were mixed in 1 g of each of those four matrices: either 1 g of distilled water, Gel 1 (Super Leaves™ Orange Leaves shower gel, ATTITUDE™, Canada), Gel 2 (and Oatmeal Sensitive Extra Gentle, ATTITUDE™, Canada) or a body cream (Super Leaves™ Orange Leaves body cream, ATTITUDE™, Canada). Samples were prepared in triplicate ($n = 3$) for each testing period and aged in ambient conditions. After 0.5, 1, 2, 3, 7, 14, 21, and 28 days, the microbeads were removed from the matrices, gently rinsed with distilled water, and dried in a vacuum oven at 50°C for 24 h to remove any residual humidity. Dried microbeads were weighed, and stability was calculated by comparing the mass of the beads before and after soaking in the sample matrices using Equation (5):

$$\text{Mass yield}(\%) = \left(\frac{W_n}{W_0}\right) \times 100, \quad (5)$$

where W_n is the weight in grams of the dried microbeads after n days and W_0 is the initial weight in grams of the beads. Mass yield (%) indicates the mass yield of beads before and after n days (in terms of %).

A further set of stability samples was prepared with 1 g of dried beads dispersed throughout 40 g of a solid glycerine soap base (by melting and resolidifying the soap). Samples were aged in ambient conditions for 3 months. Dried beads were also kept at ambient conditions for 1 year. Qualitative macroscopic observations (beads integrity and hardness) were noted throughout these experiments.

4.3.8 | Cleansing efficiency

Cleansing efficiency tests involved the use of a human test subject. This individual, one of the paper's authors, gave their informed consent to this experimentation.

The protocol for determining cleansing efficiency was adapted from Ju et al.[22] and modified for enhanced reproducibility. First, 0.3 g of beads (average diameter of 1.25 mm or 1.31 mm) or commercial natural exfoliant particles (ground walnut or coconut shells) were incorporated into 9 g of solid glycerine soap base. Then, squares of soap (3 cm^3) with and without beads were mounted on a stick attached to a swivel, which was in turn attached to a fixed surface. The word "SOAP" was written on the interior of an individual's arm with a waterproof black eyeliner pencil, as this is a flat surface of sensitive skin with little hair. The written-on skin was gently wetted and washed by the soap at a pressure defined by the swivel/stick system for 10 s (passed over 10 times by the soap). The experiment was performed in triplicate ($n = 3$). Pictures were taken of the written-on skin before and after washing with the soaps and processed with ImageJ software (black-and-white contrast processing) to determine just how efficiently the makeup was removed, with cleansing efficiency calculated using Equation (6):

$$\text{CE}(\%) = \left(\frac{A_f}{A_i}\right) \times 100 \quad (6)$$

where CE denotes cleansing efficiency, A_i is the total area in mm^2 of the crayon immediately following drawing on the sample skin and A_f is the total area in mm^2 of the remaining crayon after washing. Additionally, the same experiment was performed with synthetic skin as the written-on surface (ReelSkin silicone light tone sheet, UK). Both experiments were done in triplicate.

Cleansing efficiency was also measured in terms of the total number of swivels required to completely remove the word "SOAP" written with waterproof black eyeliner from the synthetic skin. The experiment was done in five replicates ($n = 5$). The experiment was concluded and the number of washes noted once cleansing efficiency (as determined by Equation (6)) was 100% (no eyeliner remained).

ACKNOWLEDGMENTS

This work was supported by funding from the MITACS Accelerate program, the Ministère de l'Agriculture, des Pêcheries et de l'Alimentation du Québec, and the Partenariat canadien pour l'agriculture (Innov'action grant no. IA119014). It should be mentioned that the Celova® Cellulose Powder samples (C500, C1000, and C2000) used in this study were provided free of charge by Weidmann Fiber Technology (Switzerland) and that BSG samples were donated by the Ras L'Bock and Le Bien le Malt microbreweries. We would also like to acknowledge the contributions of the Laboratoire des Technologies de la biomasse (Université de Sherbrooke), Prof. Thierry

Ghislain, and Emy Leblanc for the analysis of biomass composition; the Laboratoire de microanalyse (Université Laval), Dr. Marc Choquette, and Suzie Côté for SEM-EDS analysis; and the Laboratoire de nano-mécanique pour les matériaux de construction (Université Laval), Dr. Luca Sorelli, and Mahdiar Dargahi for microindentation testing. Additional thanks to Dr. Charles Lavigne and Charles Emond of the Centre de développement bioalimentaire du Québec for their mentorship. The authors also acknowledge the contribution of Dr. Élise Caron to the early stages of the project.

CONFLICT OF INTEREST STATEMENT

The authors declare no conflicts of interest.

ORCID

Sébastien Cardinal https://orcid.org/0000-0003-4281-2691

REFERENCES

[1] P. Corcoran, *Environ. Sci.: Processes Impacts* **2015**, *17*, 1363.
[2] C. Reed, *New Sci.* **2015**, *225*, 28.
[3] GESAMP, Sources, Fate and Effects of Microplastics in the Marine Environment: A Global Assessment, Report, IMO/FAO/UNESCO-IOC/UNIDO/WMO/IAEA/UN/UNEP/UNDP Joint Group of Experts on the Scientific Aspects of Marine Environmental Protection. **2015**.
[4] J. Frias, R. Nash, *Mar. Pollut. Bull.* **2019**, *138*, 145.
[5] M. MacLeod, H. Arp, M. Tekman, A. Jahnke, *Science* **2021**, *373*, 61.
[6] M. Browne, P. Crump, S. Niven, E. Teuten, A. Tonkin, T. Galloway, R. Thompson, *Environ. Sci. Technol.* **2011**, *45*, 9175.
[7] M. Browne, T. Galloway, R. Thompson, *Environ. Sci. Technol.* **2010**, *44*, 3404.
[8] J. Barrett, Z. Chase, J. Zhang, M. Banaszak Holl, K. Willis, A. Williams, B. Hardesty, C. Wilcox, *Front. Mar. Sci.* **2020**, *7*, 576170.
[9] L. Woodall, A. Sanchez-Vidal, M. Canals, G. Paterson, R. Coppock, V. Sleight, A. Calafat, A. Rogers, B. Narayanaswamy, R. Thompson, *Royal Soc. Open Sci.* **2014**, *1*, 140317.
[10] P. Davison, R. Asch, *Mar. Ecol.: Prog. Ser.* **2011**, *432*, 173.
[11] M. Kosuth, S. Mason, E. Wattenberg, *PLoS One* **2018**, *13*, e0194970.
[12] A. Jamieson, T. Malkocs, S. Piertney, T. Fujii, Z. Zhang, *Nat. Ecol. Evol.* **2017**, *13*, 51.
[13] V. Zitko, M. Hanlon, *Mar. Pollut. Bull.* **1991**, *22*, 41.
[14] L. Fendall, M. Sewell, *Mar. Pollut. Bull.* **2009**, *58*, 1225.
[15] K. Duis, A. Coors, *Environ. Sci. Eur.* **2016**, *28*, 2.
[16] F. Murphy, C. Ewins, F. Carbonnier, B. Quinn, *Environ. Sci. Technol.* **2016**, *50*, 5800.
[17] P. Iyare, S. Ouki, T. Bond, *Environ. Sci.: Water Res. Technol.* **2020**, *6*, 2664.
[18] E. Watkins, J.-P. Schweitzer, E. Leinala, P. Börkey, Policy Approaches to Incentivise Sustainable Plastic Design, Report, Éditions OECD, Paris. **2019**.
[19] R. Geyer, J. R. Jambeck, K. L. Law, *Sci. Adv.* **2017**, *3*, e1700782.
[20] C. Lassen, S. Hansen, K. Magnusson, N. Hartmann, P. Rehne Jensen, T. Nielsen, A. Brinch, Microplastics: Occurrence, Effects and Sources of Releases to the Environment in Denmark, Report No. 1793, The Danish Environmental Protection Agency. **2015**.
[21] J. Li, X. Qu, L. Su, W. Zhang, D. Yang, P. Kolandhasamy, D. Li, H. Shi, *Environ. Pollut.* **2016**, *214*, 177.
[22] S. Ju, G. Shin, M. Lee, J. Koo, H. Jeon, Y. Ok, D. Hwang, S. Hwang, D. Oh, J. Park, *Green Chem.* **2021**, *23*, 6953.
[23] A. Decker, E. Graber, *J. Clin. Aesthet. Dermatol.* **2012**, *5*, 32.
[24] R. Habib, M. Salim Abdoon, R. Al Megbaali, F. Ghebremedhin, M. Elkashlan, W. Kittaneh, N. Cherupurakal, A.-H. Mourad, T. Thiemann, R. Al Kindi, *Environ. Pollut.* **2020**, *258*, 113831.
[25] Z. Draelos, *Astringents, Masks, and Ancillary Skin Care Products*, 4th ed., Informa Healthcare, New York **2017**.
[26] H. C. Nam, W. H. Park, *ACS Biomater. Sci. Eng.* **2020**, *6*, 2440.
[27] S. Baek, S.-K. Moon, R. Kang, Y. Ah, H. Kim, S.-W. Choi, *Macromol. Mater. Eng.* **2018**, *303*, 223.
[28] A. Munoz-Bonilla, C. Echeverria, A. Sonseca, M. P. Arrieta, M. Fernandez-Garcia, *Materials* **2019**, *12*, 641.
[29] H. C. Nam, W. H. Park, *Int. J. Biol. Macromol.* **2019**, *157*, 734.
[30] D. S. Green, B. Boots, J. Sigwart, S. Jiang, C. Rocha, *Environ. Pollut.* **2016**, *208*, 426.
[31] C. A. King, J. L. Shamshine, O. Zavgorodnya, T. Cutfield, L. E. Block, R. D. Rogers, A. C. S. Sustain, *Chem. Eng.* **2017**, *5*, 11660.
[32] D. Elieh-Ali-Komi, M. Hamblin, *Int. J. Adv. Res.* **2016**, *4*, 411.
[33] S. Govindasamy, I. Syafiq, A. Amirul, R. Amin, K. Bhubalan, *Data Brief* **2019**, *23*, 103675.
[34] J. OBrien, L. Torrente-Murciano, D. Mattia, J. L. Scott, *ACS Sustain. Chem. Eng.* **2017**, *5*, 5931.
[35] R. Sescousse, T. Budtova, *Cellulose* **2009**, *16*, 417.
[36] P. Rosenberg, M. Rom, J. Janicki, P. Fardim, *Cellul. Chem. Technol.* **2008**, *42*, 293.
[37] A. K. Jha, A. Bhattacharya, *Asian J. Pharm. Sci.* **2009**, *3*, 299.
[38] J. Kozlowska, W. Prus, N. Stachowiak, *Int. J. Biol. Macromol.* **2019**, *129*, 952.
[39] B. Kupikowska-Stobba, D. Lewinska, *Biomater. Sci.* **2020**, *8*, 1536.
[40] M. Gericke, J. Trygg, P. Fardim, *Chem. Rev.* **2013**, *113*, 4812.
[41] S. M. K. Mohamed, K. Ganesan, B. Milow, L. Ratke, *RSC Adv.* **2015**, *5*, 90193.
[42] J. Trygg, P. Fardim, M. Gericke, E. Mäkilä, J. Salonen, *Carbohydr. Polym.* **2013**, *93*, 291.
[43] D. Tristantini, A. Yunan, *E3S Web Conf.* **2018**, *67*, 04045.
[44] T. Liebert, T. Heinze, K. Edgar, *Cellulose Solvents: For Analysis, Shaping and Chemical Modification*, ACS Symposium Series, American Chemical Society, Washington, DC **2010**.
[45] H. Sobue, H. Kiessig, K. Hess, *Z. Physik Chem* **1939**, *43*, 309.
[46] K. Gabov, T. Oja, T. Deguchi, A. Fallarero, P. Fardim, *Cellulose* **2016**, *24*, 641.
[47] C. Frangville, M. Rutkevicius, A. Richter, O. Velev, S. Stoyanov, V. Paunov, *ChemPhysChem* **2012**, *13*, 4235.
[48] R. Sescousse, A. Smacchia, T. Budtova, *Cellulose* **2010**, *17*, 1137.
[49] F. Freitas, M. Cerqueira, C. Gonçalves, S. Azinheiro, A. Garrido-Maestu, A. Vicente, L. Pastrana, J. Teixeira, M. Michelin, *Int. J. Biol. Macromol.* **2020**, *163*, 1798.
[50] M. Österberg, M. Sipponen, B. Mattos, O. Rojas, *Green Chem.* **2020**, *22*, 2712.

[51] K. Lynch, E. Steffen, E. Arendt, *J. Inst. Brew.* **2016**, *122*, 553.
[52] S. Mussatto, *J. Sci. Food Agric.* **2014**, *94*, 1264.
[53] J. Buffington, *Appl. Comput. Electromagn. Soc. J.* **2014**, *4*, 308.
[54] S. Mussatto, G. Dragone, I. Roberto, *J. Cereal Sci.* **2006**, *43*, 1.
[55] S. Aliyu, M. Bala, *Afr. J. Biotechnol.* **2011**, *10*, 324.
[56] J. Trygg, P. Fardim, *Cellulose* **2011**, *18*, 987.
[57] S. Mussatto, I. Roberto, *J. Sci. Food Agric.* **2005**, *85*, 2453.
[58] B. Matebie, B. Tizazu, A. Kadhem, S. Prabhu, *J. Nanomater.* **2021**, *2021*, 7133154.
[59] J. Rojas-Chamorro, I. Romero, J. Lopez-Linares, E. Castro, *Renewable Energy* **2020**, *148*, 81.
[60] D. Yang, T. Gao, Z. Mao, *BioResources* **2019**, *14*, 8892.
[61] Y. Wang, Cellulose Fiber Dissolution in Sodium Hydroxide Solution at Low Temperature: Dissolution Kinetics and Solubility Improvement, Thesis, Georgia Institute of Technology. **2008**.
[62] S. Väisänen, H. Kosonen, M. Ristolainen, T. Vuorinen, *Cellulose* **2021**, *28*, 4385.
[63] G. Davidson, *J. Text. Inst.* **1937**, *28*, T27.
[64] C. Roy, T. Budtova, P. Navard, *Biomacromolecules* **2003**, *4*, 259.
[65] J. Zhou, L. Zhang, *Polym. J.* **2000**, *32*, 866.
[66] M. Lara-Serrano, S. Morales-delaRosa, J. Campos-Martin, J. Fierro, *Green Chem.* **2020**, *22*, 3860.
[67] Z. Jiang, J. Fan, V. Budarin, D. Macquarrie, Y. Gao, T. Li, C. Hu, J. Clark, *Sustain* **2018**, *2*, 936.
[68] L. Zhang, D. Ruan, S. Gao, *J. Polym. Sci.* **2002**, *40*, 1521.
[69] D. F. Coutinho, A. F. Ahari, N. N. Kachouie, M. E. Gomes, N. M. Neves, R. L. Reis, A. Khademhosseini, *Biofabrication* **2012**, *4*, 035003.
[70] J. Damay, X. Duret, T. Ghislain, O. Lalonde, J.-M. Lavoie, *Ind. Crops Prod.* **2018**, *111*, 482.
[71] J. Kjeldahl, Z. Anal, *Chem* **1883**, *22*, 366.
[72] D. Waters, F. Jacob, J. Titze, E. Arendt, E. Zannini, *Eur. Food Res. Technol.* **2012**, *235*, 767.
[73] P. K. Mishra, T. Gregor, R. Wimmer, *BioResources* **2017**, *12*, 107.
[74] Q. Sun, S.-Y. Ren, H.-G. Ni, *Sci. Total Environ.* **2020**, *742*, 40218.
[75] K. Salasinska, M. Barczewski, R. Gorny, A. Klozinski, *Polymer* **2018**, *75*, 2511.
[76] N. Meneses, S. Martins, J. Teixeira, S. Mussatto, *Sep. Purif. Technol.* **2013**, *108*, 152.
[77] S. Mussatto, I. Roberto, *J. Chem. Technol. Biotechnol.* **2006**, *81*, 268.
[78] P. Miao, K. Han, Y. Tang, B. Wang, T. Lin, W. Cheng, *Nanoscale* **2015**, *7*, 1586.
[79] X. Luo, L. Zhang, *J. Chromatogr. A* **2010**, *1217*, 5922.
[80] O. El Korhani, D. Zaouk, S. Cerneaux, R. Khoury, A. Khoury, D. Cornu, *Nanoscale Res. Lett.* **2013**, *8*, 121.
[81] L. Li, T. Dong, *J. Mater. Chem. C* **2018**, *6*, 7944.
[82] S. Chichoz, A. Masek, *Materials* **2020**, *13*, 4573.
[83] S. Naduparambath, E. Purushothaman, *Cellulose* **1803**, *2016*, 23.
[84] A. Nkeumaleu, D. Benetti, M. Haddadou, I. Di Mare, C. Ouellet-Plamondon, F. Rosei, *RSC Adv.* **2022**, *12*, 11621.
[85] M. El-Sakhawy, S. Kamel, A. Salama, H.-A. Sarhan, *Cellul. Chem. Technol.* **2018**, *52*, 193.
[86] H. Qi, C. Chang, L. Zhang, *Green Chem.* **2009**, *11*, 177.
[87] A.-Y. Jee, M. Lee, *Polym. Test.* **2010**, *29*, 95.
[88] W. Li, Z. Zhai, Q. Pang, Z. Kong, Z. Zhou, *Wear* **2013**, *301*, 353.
[89] D. Manas, M. Ovsik, A. Mizera, M. Manas, L. Hylova, M. Bednarik, M. Stanek, *Polymer* **2018**, *10*, 158.
[90] G. Kaupp, M. Maimi-Jamal, *J. Mater. Chem.* **2011**, *21*, 8389.

SUPPORTING INFORMATION

Additional supporting information can be found online in the Supporting Information section at the end of this article.

How to cite this article: A. McMackin, V. Banville, S. Cardinal, *J. Polym. Sci.* **2024**, 1. https://doi.org/10.1002/pol.20230613